中國機械工程學刊第三十九卷第三期第 245~254 頁(民國一百零七年)
Journal of the Chinese Society of Mechanical Engineers, Vol.39, No.3, pp 245~254 (2018)

Displacement and Force Analyses of an Upper Limb Driving a Rehabilitation Robot Using F_R-SUC$_r$-U Model

Shen-Tarng Chiou* , Hao-Che Liou**, Ming-Shaung Ju* and Chou-Ching Ko Lin***

Keywords: upper extremity (limb), skeleton model, rehabilitation robot, displacement analysis, force analysis.

ABSTRACT

The main purpose of this study is to develop a biomechanical model of the upper extremity for analyzing joint displacements and forces of the limb when it drives a rehabilitation robot. An S-SUC$_r$-U chain is proposed as a new skeleton model (from the shoulder joint to the wrist joint) of the upper limb, which has better description of pronation/supination of forearm when the humerus is held fixed. Based on the chain, an F_R-SUC$_r$-S spatial 4-bar mechanism is proposed for simulating the upper limb driving a rehabilitation robot. The displacement model of the 4-bar mechanism is then developed and two approaches, namely, three-actuator and multi-actuator approaches are adopted for the force analysis. For each approach, computer programs are developed and the results are compared with those of using the Adams software for validation. The results revealed that the multi-actuator approach yields more reasonable results than the three-actuator approach and the objective function of the optimization problem is feasible. The net joint torques and forces can be used in solving the load sharing of the muscles of the upper extremity in next stage of research.

Paper Received December, 2015. Revised August, 2017. Accepted November, 2017. Author for Correspondence: Shen-Tarng Chiou

* *Professor, Department of Mechanical Engineering, National Cheng Kung University, Tainan City, Taiwan 701.*
** *Engineer, Department of R & D, JIH-I Machinery Co., Ltd., Taichung City, Taiwan 420.*
*** *Professor, Department of Neurology, National Cheng Kung University, Tainan City, Taiwan 701.*

INTRODUCTION

There are equipments interact with the upper limbs, for example, wheelchair, exercise trainers, and the rehabilitation robots. For better designs of these devices, appropriate models of the upper limb should be developed and the interaction with these devices has to be analyzed to obtain the joint motions, joint torques and muscle forces. Using the kinematic and kinetic data, better design of above-mentioned devices may be achieved. Compared with the joints in mechanical systems, the kinematic and kinetic analyses of the upper extremity is quite challenging due to complicated geometry of the joints and the number of muscles is much greater than that of degree of freedom of the upper extremity.

Regarding the skeletal model involving the shoulder, arm, forearm and hand of an upper limb, Lemay and Crago (1996) used a spatial RCS-U kinematic chain for the skeleton and Hill-type muscles and applied the software Adams to analyze its kinematics, muscle forces and muscle lengths. Fazel-Rezai, *el al*. (1996) instrumented 6 markers on the upper limb of subjects and built a kinematic model which had 3, 2 and 2 degrees of freedom (DOF) for the shoulder, elbow, and wrist, respectively, according to the data collected. Holzbaur, *et al*. (2005) developed a model of the upper extremity that has 15 DOFs including the shoulder, elbow, forearm, wrist, thumb, and index finger, and 50 muscles across these joints and estimated the muscle–tendon lengths and moment arms for all the muscles over some postures. Nunome, *et al*. (2002) placed reflective markers at anatomical landmarks of the upper limb, and videotaped tetraplegic wheelchair basketball players, to investigate their shooting abilities when compared with those of the able players.

Zhou, *et al*. (2006) suggested an upper limb model with a kinematic chain in which three joint variables are considered for the shoulder joint and one for the elbow joint; based on inertial measurements of the wrist motion, to develop a motion tracking device that can be integrated within a home-based rehabilitation system for stroke patients. Pennestrı`, *et al*. (2007) proposed a musculo-skeletal model of the upper limb with a 7 DOF spatial mechanism and 24 muscles. Based on kinematic analysis model and minimum effort principle, they can find the activation coefficients of all muscles. Gattamelata, *et al*. (2007) derived a set of equations for simulating joints of the upper limb segments and embedded in a virtual environment for simulating relative motion among body segments.

For the studies of wheelchair propulsion, Wu, *et al*. (1998) developed an instrumented wheel system for kinetic analysis of upper limb. The system was applied to measure the forces and torques of the upper limb acting on the hand rim and to investigate the motions and loads of the shoulder, elbow and wrist (1998). Garner and Pandy (1999) used high-resolution medical images to develop a kinematic model of the upper limb including seven joints with a total of 13 DOFs and 26 muscles. The positions and orientations of all joint axes and the bone-fixed reference frames were reported.

Mercer, *et al*. (2006) recorded the kinematic and kinetic data of 33 subjects with paraplegia as they propelled their wheelchairs at two speeds to examine the relationship between shoulder forces and torques experienced during wheelchair propulsion and shoulder pathology. Chen and Chiou (2013a) proposed a RUUS skeletal model to simulate an upper limb propelling a wheelchair, and derived the closed-form solution of its displacement analysis. They (Chen and Chiou, 2013b) also built the static force analysis model and tested three objective functions, namely, the driving torques, relative discomfort, or ergonomic index, for searching the optimal motor control of the manual wheelchair propulsion.

Regarding the studies of developing the rehabilitation robots, Chen (2000) developed a robot, installed sensors to measure joint displacement and reactive forces, for rehabilitation of patients with neuro-muscular disorders by performing various facilitation patterns. Wu (2003) employed the robot to perform various treatment protocols on stroke patients and designed a subsystem for measuring rotary torque of the forearm and an EMG measuring system. Kung, *et al*. (2007) designed a robot for assisting forearm rehabilitation of patients with neuromuscular disorders by guiding subject's forearm to pronate/supinate along planned saw-tooth or ramp-and-hold trajectories under passive mode or active mode.

The main purpose of this study is to propose a skeleton of the upper extremity and develop models to analyze the joint displacements, torques and forces of the upper limb when it drives the rehabilitation robot (Kung, *et al*., 2007). In particular, an S-SUCr-U chain is proposed as a novel skeleton model (from the shoulder joint to the wrist joint) of the upper limb. Based on the model, an F_R-SUCr-S spatial 4-bar mechanism is proposed for simulating the upper limb driving the rehabilitation robot. By using the homogeneous transformation matrices, the displacement model is then developed; consequently, two models, 3 actuator model and multi-actuator model, are built for the force analysis. The results are to be verified by those of using the Adams software. The results of two force analyses are compared and discussed on which one is more reasonable.

SKELETAL MODELS

The human upper limb consists of three segments, namely upper-arm, fore-arm, and hand. For simplicity, the radius and ulna in the forearm was treated as a single link in previous studies. Although both of the skeletal models proposed by Lemay and Crago (1996), and Pennestrı` *et al* (2007) do consider radius and ulna as seperate bones but the forearm could not perform pronation and supination motions when the upper arm was held fixed. It is necessary to develop a model which allows pronation/supination.

A spatial S-SUCr-U kinematic chain shown in Fig. 1 is proposed as the skeletal model between the shoulder and hand of an upper limb. The joints between scapula and humerus, humerus and radius, humerus and ulna, radius and ulna, and radius and hand are considered as spherical (S), spherical, universal (U), cylindrical and revolute (Cr), and universal joints, respectively. In particular, the Cr joint between the radius and ulna is an integration of a cylindrical and a revolute joint and thus it has 3 DOFs.

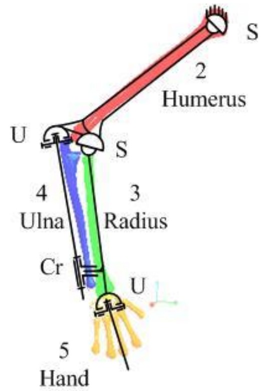

Fig. 1 S-SUCr-U skeletal model of an upper limb

When the upper arm is held fixed, a rotational axis, of the universal joint between the humerus and ulna, passes through the spherical-joint-center between the humerus and radius, to allow elbow flexion/extension.

The other rotational axis is perpendicular to the line between two joints on the ulna so that the forearm is able to do pronation/supination when the upper arm is held fixed. Hence, this new model give better descriptions of the forearm motions.

Kung, *et al* (2007) built a rehabilitation robot, whose photographs are as shown in Fig. 2. When the shoulder is held fixed, the elbow and wrist are kept at the same height, and the upper limb, whose hand is clamped within the end-effecter of the robot, drives the robot, as shown in Fig. 2, then the relative motions between the wrist and the frame of the robot have four DOFs (two rotations and two translations); and an F_R joint (which is a planar joint integrated with a revolute joint) is used to simulate it. Thus the F_R-SUCr-S spatial four bar mechanism, whose schematic diagram is shown in Fig. 3, is proposed as the skeletal model of the upper limb driving the rehabilitation robot. The humerus, radius, and ulna are designated as links 2, 3, and 4, respectively.

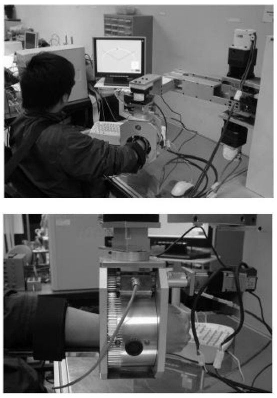

Fig. 2 Rehabilitation robot (Kung, *et al*, 2007)

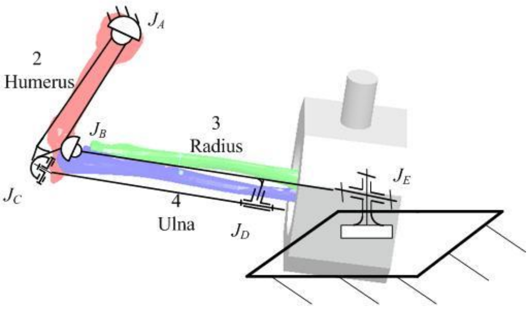

Fig. 3 F_R-SUCr-S spatial four bar mechanism

DISPLACEMENT ANALYSIS

In order to develop the model for the displacement analysis of the F_R-SUCr-S spatial four bar mechanism, firstly, 19 coordinate systems are defined on links; sencondly, loop closure equations are derived, whose solutions are the angular and translational displacements of the joints; furthermore, the positions of centers of gravity of links can also be determined and used in joint force analysis.

As shown in Fig. 4, the origins of coordinates $\mathbf{X}_0\mathbf{Y}_0\mathbf{Z}_0$ ~ $\mathbf{X}_3\mathbf{Y}_3\mathbf{Z}_3$ are all located at the center of shoulder joint, J_A, where $\mathbf{X}_0\mathbf{Y}_0\mathbf{Z}_0$ is the reference coordinate system, and $\mathbf{X}_1\mathbf{Y}_1\mathbf{Z}_1$ ~ $\mathbf{X}_3\mathbf{Y}_3\mathbf{Z}_3$ are moving coordinate systems. Rotating $\mathbf{X}_0\mathbf{Y}_0\mathbf{Z}_0$ with an angle θ_1 about $\mathbf{Z}_0$ axis gives $\mathbf{X}_1\mathbf{Y}_1\mathbf{Z}_1$. Rotating $\mathbf{X}_1\mathbf{Y}_1\mathbf{Z}_1$ with an angle θ_2 about $\mathbf{X}_1$ axis gives $\mathbf{X}_2\mathbf{Y}_2\mathbf{Z}_2$. Rotating $\mathbf{X}_2\mathbf{Y}_2\mathbf{Z}_2$ with an angle θ_3 about $\mathbf{Z}_2$ axis gives $\mathbf{X}_3\mathbf{Y}_3\mathbf{Z}_3$, which is the moving coordinate system attached to humerus.

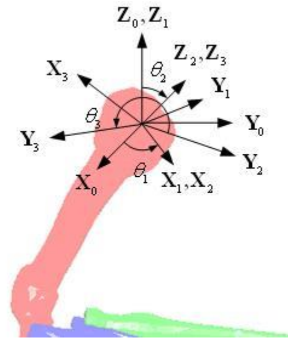

Fig.4 Coordinate systems on the shoulder joint

As shown in Fig. 5, the origins of coordinates $\mathbf{X}_4\mathbf{Y}_4\mathbf{Z}_4$ ~ $\mathbf{X}_7\mathbf{Y}_7\mathbf{Z}_7$ are all located at the joint center between humerus and radius, J_B. The homogeneous transformation matrix from $\mathbf{X}_3\mathbf{Y}_3\mathbf{Z}_3$ to $\mathbf{X}_4\mathbf{Y}_4\mathbf{Z}_4$ is ${}^4\mathbf{M}_3$, which not only translates its origin to J_B but also makes $\mathbf{X}_4$ along with rotational axis for elbow flexion. Rotating $\mathbf{X}_4\mathbf{Y}_4\mathbf{Z}_4$ with an angle θ_4 about $\mathbf{X}_4$ axis gives $\mathbf{X}_5\mathbf{Y}_5\mathbf{Z}_5$. Rotating $\mathbf{X}_5\mathbf{Y}_5\mathbf{Z}_5$ with an angle θ_5 about $\mathbf{Y}_5$ axis gives $\mathbf{X}_6\mathbf{Y}_6\mathbf{Z}_6$. Rotating $\mathbf{X}_6\mathbf{Y}_6\mathbf{Z}_6$ with an angle θ_6 about $\mathbf{Z}_6$ axis gives $\mathbf{X}_7\mathbf{Y}_7\mathbf{Z}_7$, which is the moving coordinate system attached to the radius.

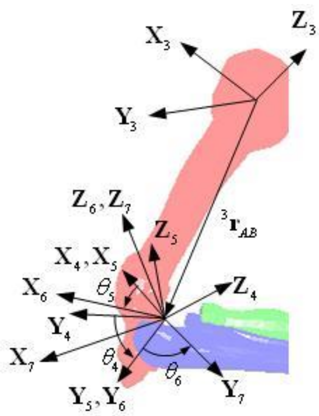

Fig. 5 Coordinate systems on the joint between humerus and radius

As shown in Fig. 6, the origins of coordinates $\mathbf{X}_8\mathbf{Y}_8\mathbf{Z}_8$~ $\mathbf{X}_{12}\mathbf{Y}_{12}\mathbf{Z}_{12}$ are all located at the wrist joint center, J_E. Translating $\mathbf{X}_7\mathbf{Y}_7\mathbf{Z}_7$ with vector ${}^7\mathbf{r}_{BE} = [{}^7r_{BEx}\ {}^7r_{BEy}\ {}^7r_{BEz}]^T$ gives $\mathbf{X}_8\mathbf{Y}_8\mathbf{Z}_8$. Rotating $\mathbf{X}_8\mathbf{Y}_8\mathbf{Z}_8$ with an angle θ_{11} about $\mathbf{Z}_8$ axis gives $\mathbf{X}_9\mathbf{Y}_9\mathbf{Z}_9$. Rotating $\mathbf{X}_9\mathbf{Y}_9\mathbf{Z}_9$ with -90° about X_9 axis then rotating with an angle θ_{12} about $\mathbf{Z}_{10}$ axis gives $\mathbf{X}_{10}\mathbf{Y}_{10}\mathbf{Z}_{10}$. Translating $\mathbf{X}_{10}\mathbf{Y}_{10}\mathbf{Z}_{10}$ with vector $\mathbf{r}_1$, which is the position vector of J_E with respect to $\mathbf{X}_0\mathbf{Y}_0\mathbf{Z}_0$ and can be measured. It can be noted that θ_{11} and θ_{12} are the angulur displacements of the wrist.

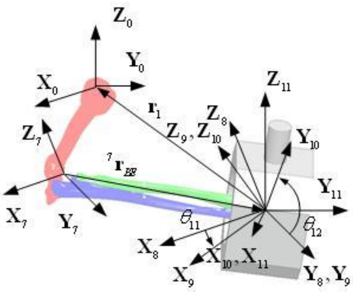

Fig. 6 Coordinate systems on the wrist

As shown in Fig. 7, the origins of coordinates $\mathbf{X}_{13}\mathbf{Y}_{13}\mathbf{Z}_{13}$~ $\mathbf{X}_{15}\mathbf{Y}_{15}\mathbf{Z}_{15}$ are all located at the joint center between humerus and ulna, J_C. The homogeneous transformation matrix from $\mathbf{X}_3\mathbf{Y}_3\mathbf{Z}_3$ to $\mathbf{X}_{13}\mathbf{Y}_{13}\mathbf{Z}_{13}$ is ${}^{13}\mathbf{M}_3$, which not only translates its origin to J_C but also makes $\mathbf{X}_{13}$ along with rotational axis for elbow flexion. Rotating $\mathbf{X}_{13}\mathbf{Y}_{13}\mathbf{Z}_{13}$ with an angle θ_7 about $\mathbf{X}_{13}$ axis gives $\mathbf{X}_{14}\mathbf{Y}_{14}\mathbf{Z}_{14}$. Rotating $\mathbf{X}_{14}\mathbf{Y}_{14}\mathbf{Z}_{14}$ with an angle θ_8 about $\mathbf{Y}_{14}$ axis gives $\mathbf{X}_{15}\mathbf{Y}_{15}\mathbf{Z}_{15}$, which is the moving coordinate system attached to the ulna. θ_7 and θ_8 are the angulur displacements of the joint between humerus and ulna.

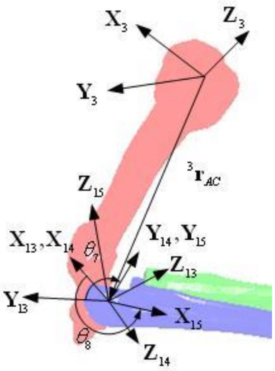

Fig. 7 Coordinate systems on the joint between humerus and ulna

As shown in Fig. 8, the origins of coordinates $\mathbf{X}_{16}\mathbf{Y}_{16}\mathbf{Z}_{16}$ and $\mathbf{X}_{17}\mathbf{Y}_{17}\mathbf{Z}_{17}$ are both located at the joint center between ulna and radius, J_D. Translating $\mathbf{X}_{15}\mathbf{Y}_{15}\mathbf{Z}_{15}$ with vector ${}^{15}\mathbf{r}_{CD}$ gives $\mathbf{X}_{16}\mathbf{Y}_{16}\mathbf{Z}_{16}$. Rotating $\mathbf{X}_{16}\mathbf{Y}_{16}\mathbf{Z}_{16}$ with an angle θ_9 about $\mathbf{Z}_{16}$ axis gives $\mathbf{X}_{17}\mathbf{Y}_{17}\mathbf{Z}_{17}$. Translating $\mathbf{X}_{17}\mathbf{Y}_{17}\mathbf{Z}_{17}$ with $-h_D$ along with $\mathbf{Y}_{17}$ gives $\mathbf{X}_{18}\mathbf{Y}_{18}\mathbf{Z}_{18}$. Rotating $\mathbf{X}_{18}\mathbf{Y}_{18}\mathbf{Z}_{18}$ with an angle θ_{10} about $\mathbf{Y}_{18}$ axis gives $\mathbf{X}_{19}\mathbf{Y}_{19}\mathbf{Z}_{19}$, which is the other moving coordinate system attached to the radius, and its 3 axes are parallel to those of $\mathbf{X}_7\mathbf{Y}_7\mathbf{Z}_7$, respectively. It can be noted that θ_9 and θ_{10} are the angular displacements of the joint between ulna and radius, and h_D is the linear diaplacement.

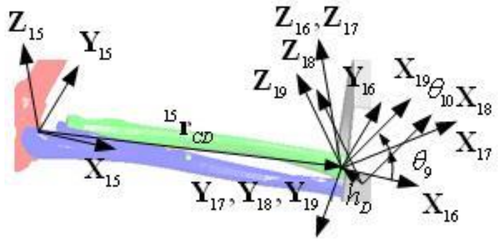

Fig. 8 Coordinate systems on the joint between ulna and radius

As shown in Fig. 9, translating $\mathbf{X}_{19}\mathbf{Y}_{19}\mathbf{Z}_{19}$ with vector $-{}^7\mathbf{r}_{BD}$ gives $\mathbf{X}_7\mathbf{Y}_7\mathbf{Z}_7$. Rotating $\mathbf{X}_7\mathbf{Y}_7\mathbf{Z}_7$ with angles $-\theta_6$ ~ $-\theta_4$ gives $\mathbf{X}_4\mathbf{Y}_4\mathbf{Z}_4$. Translating $\mathbf{X}_4\mathbf{Y}_4\mathbf{Z}_4$ with (${}^3\mathbf{r}_{AC}$ $-{}^3\mathbf{r}_{AB}$) gives $\mathbf{X}_{13}\mathbf{Y}_{13}\mathbf{Z}_{13}$. Cossequently, there are two loop closure eqations within this mechanism, which are:

$${}^{0}\mathbf{M}_{10}\,{}^{10}\mathbf{M}_{9}\,{}^{9}\mathbf{M}_{8}\,{}^{8}\mathbf{M}_{7}\,{}^{7}\mathbf{M}_{6}\,{}^{6}\mathbf{M}_{5}\,{}^{5}\mathbf{M}_{4}\,{}^{4}\mathbf{M}_{3}\,{}^{3}\mathbf{M}_{2}\,{}^{2}\mathbf{M}_{1}\,{}^{1}\mathbf{M}_{0}-\mathbf{I}=\mathbf{0}, \qquad (1)$$

$${}^{13}\mathbf{M}_{4}\,{}^{4}\mathbf{M}_{7}\,{}^{7}\mathbf{M}_{19}\,{}^{19}\mathbf{M}_{18}\,{}^{18}\mathbf{M}_{17}\,{}^{17}\mathbf{M}_{16}\,{}^{16}\mathbf{M}_{15}\,{}^{15}\mathbf{M}_{14}\,{}^{14}\mathbf{M}_{13}-\mathbf{I}=\mathbf{0}, \qquad (2)$$

where ${}^j\mathbf{M}_i$ is the homogeneous transformation matrix from coordinate i to coordinate j, which can be found in Liu (2011).

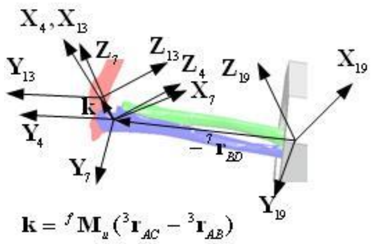

Fig. 9 Coordinate systems on radius

${}^0\mathbf{r}_{AB}$ and ${}^0\mathbf{r}_{AC}$ are vectors pointing from the shoulder joint center, J_A, to the joint center between humerus and radius, J_B, and to the joint center between ulna and radius, J_C, respectively. Similrly, ${}^0\mathbf{r}_{BD}$ and ${}^0\mathbf{r}_{BE}$ are vectors pointing from J_B, to J_D and J_E, respectively; and ${}^0\mathbf{r}_{CD}$ is the vector pointing from J_C to J_D. As shown in Fig. 6, the position vector of the wrist joint center, with respect to the reference coordinate system $\mathbf{X}_0\mathbf{Y}_0\mathbf{Z}_0$, is $\mathbf{r}_1 = [\, r_{1x}\ r_{1y}\ r_{1z}\,]^{\mathrm{T}}$, where r_{1x} and r_{1y} are to be measured by using two cameras, and r_{1z} is a specified constant. Based on the Kutzbach criterion (Waldron and Kinzel, 2004), the mechanism has 3 DOFs. r_{1x} and r_{1y} measured are its two inputs, and θ_{11} is specified as the other input. There are 12 independent simultaneous equations within Eqs. (1) and (2), with 12 unknown variables $\theta_1 \sim \theta_{10}$, θ_{12} and h_D. Consequently, the mass center locations of moving links can also be determined after these variables have been solved.

JOINT FORCE ANALYSIS

In this section, models for analyzing joint forces and torques are developed based on the Cartesian coordinate system. The $\mathrm{F_R}$-SUCr-S four bar mechanism has 3 DOFs and three inputs are sufficient to drive the mechanism to perform a constrained motion. For comparison, two approaches for force analyses are performed, namely with three actuators and with multiple actuators. In the models, the joint frictional forces are neglected as the rehabilitation robot is operated under very low speed and the inertial forces and inertial torques can also be neglected.

Equations of Motion

In the free body diagram of link 2 (humerus) as shown in Fig. 10, $\mathbf{F}_{ij}$ and $\mathbf{T}_{ij}$ are force and torque that link i acting on link j, respectively; m_2 is the mass of the upper arm. The force and torque (with respect to J_A) equilibrium equations are as follows:

$$\mathbf{F}_{12} + \mathbf{F}_{32} + \mathbf{F}_{42} + m_2\mathbf{g} = \mathbf{0}\,, \tag{3}$$

$$\mathbf{T}_{12} + \mathbf{T}_{32} + \mathbf{T}_{42} + ({}^0\mathbf{r}_{AB} \times \mathbf{F}_{32} + {}^0\mathbf{r}_{AC} \times \mathbf{F}_{42} + {}^0\mathbf{r}_{2m} \times m_2\mathbf{g}) = \mathbf{0}\,. \tag{4}$$

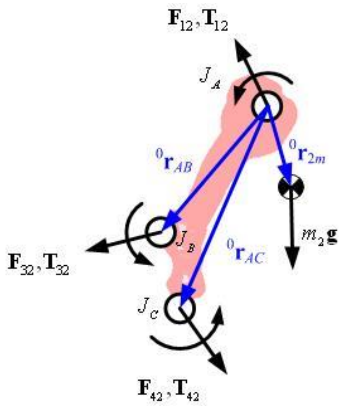

Fig. 10 Free body diagram of humerus (link 2)

The free body diagram of link 4 (ulna) is shown in Fig. 11, where m_4 is partial mass of the fore-arm attached with ulna. The force and torque (with respect to J_C) equilibrium equations are as follows:

$$-\mathbf{F}_{42} - \mathbf{F}_{43} + m_4\mathbf{g} = \mathbf{0}\,, \tag{5}$$

$$-\mathbf{T}_{42} - \mathbf{T}_{43} + (-{}^0\mathbf{r}_{CD} \times \mathbf{F}_{43} + {}^0\mathbf{r}_{4m} \times m_4\mathbf{g}) = \mathbf{0}\,. \tag{6}$$

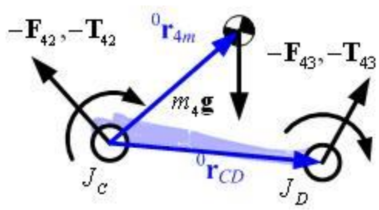

Fig. 11 Free body diagram of ulna (link 4)

The free body diagram of link 3 (radius) is shown in Fig. 12, where m_3 is the other part of mass of the fore-arm attached with radius. The force and torque (with respect to J_B) equilibrium equations are as follows:

$$-\mathbf{F}_{32} + \mathbf{F}_{43} + \mathbf{F}_{13} + \mathbf{F}_d + m_3\mathbf{g} = \mathbf{0}\,, \tag{7}$$

$$-\mathbf{T}_{32} + \mathbf{T}_{43} + \mathbf{T}_{13} + \mathbf{T}_d + [\,{}^0\mathbf{r}_{BD} \times \mathbf{F}_{43} + {}^0\mathbf{r}_{BE} \times (\mathbf{F}_{13} + \mathbf{F}_d) + {}^0\mathbf{r}_{3m} \times m_3\mathbf{g}] = \mathbf{0}\,, \tag{8}$$

where $\mathbf{F}_d$ and $\mathbf{T}_d$ are the force and torque that the robot acts on the wrist, respectively.

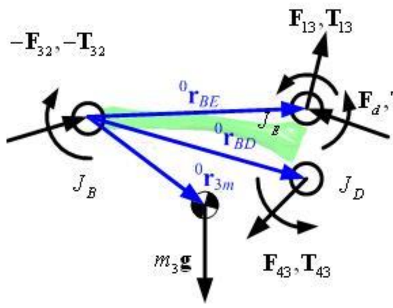

Fig. 12 Free body diagram of radius (link 3)

Joint Constrained Equations

Based on the assumptions of frictionless joints, the joint forces and torques along movable directions should have zero values, if no input torque or input force given along them. So that the torques along three rotational axes of the spherical joint at J_A should all be zero, i.e.,

$$\mathbf{T}_{12} \cdot {}^0\mathbf{Z}_0 = 0\,, \tag{9}$$

$$\mathbf{T}_{12} \cdot {}^0\mathbf{X}_1 = 0\,, \tag{10}$$

$$\mathbf{T}_{12} \cdot {}^0\mathbf{Z}_2 = 0\,. \tag{11}$$

Similarly, for those of the spherical joint at J_B, we have

$$\mathbf{T}_{32} \cdot {}^{0}\mathbf{X}_{5} = 0 \,, \tag{12}$$

$$\mathbf{T}_{32} \cdot {}^{0}\mathbf{Y}_{6} = 0 \,, \tag{13}$$

$$\mathbf{T}_{32} \cdot {}^{0}\mathbf{Z}_{7} = 0 \,. \tag{14}$$

For the two rotational axes of the universal joint at J_C, the torques along them should also be zero, i.e.,

$$\mathbf{T}_{42} \cdot {}^{0}\mathbf{X}_{13} = 0 \tag{15}$$

$$\mathbf{T}_{42} \cdot {}^{0}\mathbf{Y}_{14} = 0 \,. \tag{16}$$

Cr joint at J_D allows two rotations and one translation, the torques and force along these axes are zero, which give:

$$\mathbf{T}_{43} \cdot {}^{0}\mathbf{Z}_{16} = 0 \,, \tag{17}$$

$$\mathbf{F}_{43} \cdot {}^{0}\mathbf{Y}_{17} = 0 \,, \tag{18}$$

$$\mathbf{T}_{43} \cdot {}^{0}\mathbf{Y}_{18} = 0 \,. \tag{19}$$

There are two rotations and two translations allowed within the F_R joint at J_E. In order that the torques and forces along their axes are zero, the following relations should be satisfied:

$$\mathbf{T}_{13} \cdot {}^{0}\mathbf{Z}_{8} = 0 \,, \tag{20}$$

$$\mathbf{T}_{13} \cdot {}^{0}\mathbf{Y}_{9} = 0 \,, \tag{21}$$

$$\mathbf{F}_{13} \cdot {}^{0}\mathbf{Y}_{10} = 0 \,, \tag{22}$$

$$\mathbf{F}_{13} \cdot {}^{0}\mathbf{X}_{10} = 0 \,. \tag{23}$$

Three-actuator Approach

The F_R-SUCr-S spatial four bar mechanism has three DOFs. If three of the movable directions of joints are given with driving torques or forces, i.e., they are chosen as the inputs, then the mechanism can move with a constrained motion. Except the equations corresponding to three chosen inputs, there are 12 constrained equations remained among Eqs. (9) ~ (23), which need be satisfied. Since Eqs. (3) ~ (8) have three components, therefore totally there are 18 equilibrium equations. Thus 30 simultaneous equations can be solved for 30 unknown variables, which are F_{12x}, F_{12y}, F_{12z}, T_{12x}, T_{12y}, T_{12z}, F_{32x}, F_{32y}, F_{32z}, T_{32x}, T_{32y}, T_{32z}, F_{43x}, F_{43y}, F_{43z}, T_{43x}, T_{43y}, T_{43z}, F_{13x}, F_{13y}, F_{13z}, T_{13x}, T_{13y}, T_{13z}, F_{42x}, F_{42y}, F_{42z}, T_{42x}, T_{42y} and T_{42z}. If the solution exists then it must be unique although it may not be feasible biomechanically.

Multi-actuator Approach

In general, all joints are actuated simultaneously by their relevant muscles. Thus in this case for the F_R-SUCr-S spatial four bar mechanism, all the joints are driven by their relevant muscles, and the number of inputs is greater than the DOFs of the mechanism. An optimization problem is formulated for the load analyses in the followings.

Objective Function and Variables

The objective function, J, consists of weighted sum of the squares of the resultant forces and torques given by:

$$\min \mathrm{J} = s_1^2 w_1 F_{43}^2 + w_2 T_{12}^2 + w_3 T_{32}^2 + w_4 T_{43}^2 + w_5 T_{42}^2 \,, \tag{24}$$

where T_{ij} is the magnitudes of $\mathbf{T}_{ij}$, w_1 ~ w_5 are the weighting factors; and s_1 is the regulating factor for adjusting the magnitude order of F_{43}. The design variables are components of the forces and torques, namely, F_{12x}, F_{12y}, F_{12z}, T_{12x}, T_{12y}, T_{12z}, F_{32x}, F_{32y}, F_{32z}, T_{32x}, T_{32y}, T_{32z}, F_{43x}, F_{43y}, F_{43z}, T_{43x}, T_{43y}, T_{43z}, F_{42x}, F_{42y}, F_{42z}, T_{42x}, T_{42y} and T_{42z}. The total number of the design variables are 24 in the problem.

Constraints

When the wrist is held by the rehabilitation robot, the force and torque (with respect to J_B) equilibrium equations of link 3 should be modified as follows:

$$-\mathbf{F}_{32} + \mathbf{F}_{43} + \mathbf{F}_{d} + m_3\mathbf{g} = \mathbf{0} \,, \tag{25}$$

$$-\mathbf{T}_{32} + \mathbf{T}_{43} + \mathbf{T}_{d} + [{}^{0}\mathbf{r}_{BD} \times \mathbf{F}_{43} + {}^{0}\mathbf{r}_{BE} \times \mathbf{F}_{d} + {}^{0}\mathbf{r}_{3m} \times m_3\mathbf{g}] = \mathbf{0} \,, \tag{26}$$

where $\mathbf{F}_d$ and $\mathbf{T}_d$ are the force and torque that the rehabilitation robot acts on the wrist. In addition to above equations, the force and torque equilibrium equations of other links, i.e., Eqs. (3) ~ (6) have to be satisfied. Since these equations are vector equations so the total number of equality constraint equations is 18.

EXAMPLES

To demonstrate applicability of the model developed in this study, displacement analysis and force analysis of the upper limb driving the rehabilitation robot are given in the followings. In particular, the results of using two approaches to the force analysis will be compared and discussed.

Displacement Analysis

The F_R-SUCr-S spatial four-bar mechanism has two closed loops or chains. Matlab is adopted to develop the code on a PC for the displacement analysis of the mechanism, furthermore the Adams software is applied to verify the correctness of the results.

According to the bone dimensions given in Garner and Pandy (1999), the position vectors (from joint to joint) with respect to the local coordinates, as shown in Figs. 5 ~ 9, are as follows: on link 2, ${}^{3}\mathbf{r}_{AB}$ = [23.85 25.19

-297.21]^T and $^3\mathbf{r}_{AC}$ = [0.81 25.18 -303.29]^T; on link 3, $^7\mathbf{r}_{BD}$ = [-18.34 -0.34 -278.11]^T and $^7\mathbf{r}_{BE}$ = [16.65 6.33 -283.46]^T; and on link 4, $^{15}\mathbf{r}_{CD}$ = [-19.63 -0.35 -282.94]^T; regarding the position vectors of the mass centers of links 2, 3 and 4 are $^3\mathbf{r}_{2m}$ = [-5.47 8.88 -125.73]^T, $^7\mathbf{r}_{3m}$ = [-6.12 9.79 -152.91]^T, and $^{15}\mathbf{r}_{4m}$ = [7.08 -12.51 -89.33]^T, respectively. If the weight of the operator, m_u, is 75 kg, according to the data given in Shan and Bohn [18], $m_2 = t_u \times m_u$, $m_3 = 0.5 \times t_f \times m_u$, and $m_4 = 0.5 \times t_f \times m_u$, where $m_2 \sim m_4$ are the masses attached to links 2 ~ 4, respectively; and t_u = 0.028, and t_f = 0.016.

Due to the Z component of the wrist is kept at zero position, so r_{1z} = 0 (mm). Two cameras are employed to measure the X and Y components of the wrist center positions, which are r_{1x} and r_{1y}, respectively. From the measured data, the path of the wrist center is shown in Fig. 13. It is specified that the relation between the angle θ_{11} and time is given by:

$$\theta_{11} = -93.50 - 50 \cdot \frac{8.88}{2\pi} \sin\left(\frac{2\pi t}{8.88}\right), \tag{27}$$

where t is time, and it takes 8.88 seconds to complete the motion with wrist center path shown in Fig. 13, and the constant term is the initial position of θ_{11}. By using θ_{11} and measured r_{1x} and r_{1y} as the inputs, and solving Eqs. (1) and (2) simultaneously, trajectories of θ_1 to θ_{10}, θ_{12} and h_D can be determined. Furthermore, the Adams software is also employed to build a solid model of the mechanism, and then displacement analyses are performed. The results of θ_{10} of both approaches are compared in Fig. 14. Due to the limitation of the paper length, other results are compared in Liu's thesis (2011). It can be found that the deviations between the results are acceptable and which verifies correctness of the displacement model and computer code.

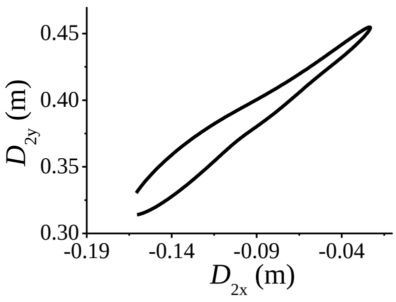

Fig. 13 Path of the wrist

Three-actuators Approach

The rehabilitation robot is installed with force sensors to measure the X and Y components of force $\mathbf{F}_d$ that the rehabilitation robot acts on the wrist. It is also assumed that the Z component of $\mathbf{F}_d$ is one third of the weight of the upper limb, i.e., ($m_2 + m_3 + m_4$)g / 3, and components of the torque are $^7T_{dx}$ = 0, $^7T_{dy}$ = 0, and $^7T_{dz}$ = sin($2\pi t$/8.88) Nm, respectively. These force and torque components are used as the loads on the mechanism for the force analysis.

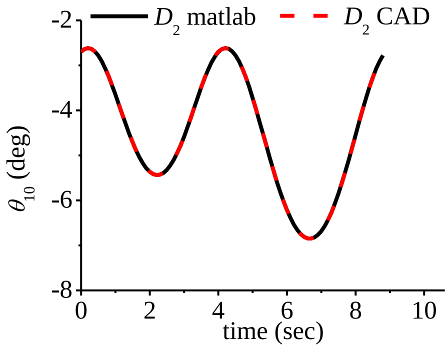

Fig. 14 θ_{10} verses time

The spatial F_R-SUCr-S mechanism has 3 DOFs, i.e., three actuators are sufficient to drive the mechanism to move with a constrained motion. If there are three actuators driving the spherical joint (which has three rotational DOF) on the shoulder, then the joint constraint equations of the shoulder joint, Eqs. (9) ~ (11), should not be considered. Based on results of the displacement analysis and the applied loads on the mechanism, Eqs. (3) ~ (8) (each has three components, and totally 18 equations) and Eqs. (12) ~ (23) (totally 12 joint constraint equations), the forces and torques of the joints can be determined, their components are F_{12x}, F_{12y}, F_{12z}, T_{12x}, T_{12y}, T_{12z}, F_{32x}, F_{32y}, F_{32z}, T_{32x}, T_{32y}, T_{32z}, F_{43x}, F_{43y}, F_{43z}, T_{43x}, T_{43y}, T_{43z}, F_{13x}, F_{13y}, F_{13z}, T_{13x}, T_{13y}, T_{13z}, F_{42x}, F_{42y}, F_{42z}, T_{42x}, T_{42y} and T_{42z}. Among the results, trajectories of components of $\mathbf{F}_{42}$ and $\mathbf{T}_{42}$ are as shown in Figs. 15 and 16, respectively. The Adams software is also applied to analyze the joint forces and torques, the curves of the relevant results are also given on both figures. It can be noted that the results of both approaches agree well with each other.

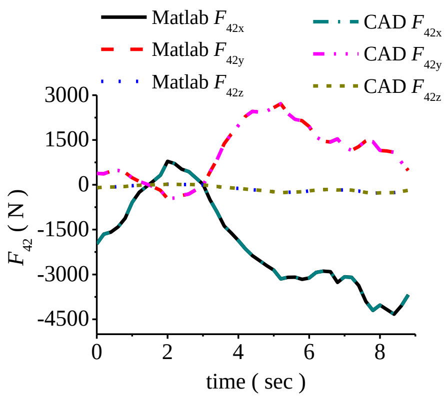

Fig. 15 Components of F_{42}

In order to test whether the results of the approach are reasonable, the loads are increased to 1.5 and 2 folds, respectively, and the problems are re-analyzed. Among the results, the curves of those of $\mathbf{F}_{32}$ and $\mathbf{T}_{32}$ with different loads are shown in Figs. 17 and 18, respectively. The magnitudes of $\mathbf{F}_{32}$ as shown in Fig. 17 are not always increased proportional to the increase of loads. Note that in Fig. 18 $\mathbf{T}_{32}$ are equal to zero even when different loads are applied. These results contradict with kinesiology of the movement. Different combinations of three actuators have also been chosen as inputs for the force analysis, and the results contradict with kinesiology of the movement (Liu, 2011). One may find that the three-actuator approach is not feasible for biomechanics of the upper limb although mathematically it does yield a unique solution.

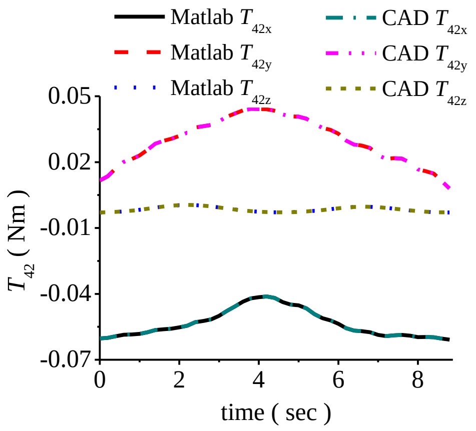

Fig. 16 Components of T_{42}

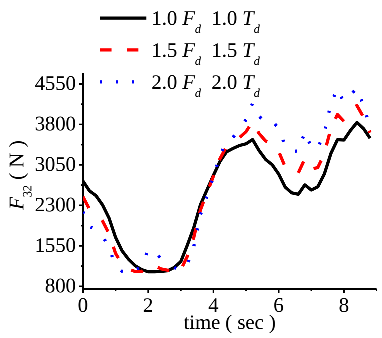

Fig. 17 Components of F_{32} with different loads

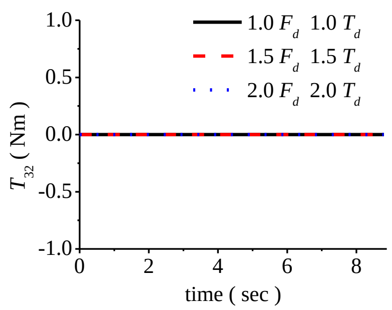

Fig. 18 Components of T_{32} with different loads

Multi-actuator Approach

If all the movable directions of the joints are driven by their actuators (muscles), then there are 24 variables, which are F_{12x}, F_{12y}, F_{12z}, T_{12x}, T_{12y}, T_{12z}, F_{32x}, F_{32y}, F_{32z}, T_{32x}, T_{32y}, T_{32z}, F_{43x}, F_{43y}, F_{43z}, T_{43x}, T_{43y}, T_{43z}, F_{42x}, F_{42y}, F_{42z}, T_{42x}, T_{42y} and T_{42z}, needed be determined. Eq. (24) is the objective function, which is a quadratic function of the variables, to be minimized. There are 18 equality constraints, which are the component equations of Eqs. (3) ~ (6), (25) and (26), and they are all linear with respect to the variables. Thus the problem is a quadratic programming (QP) problem. The function of "quadprog" in Matlab is used to solve the problem.

The same loads acting on the wrist, as given in previous section, are also adopted for the multiple-actuator approach. The weights of the objective function J are specified as followings: s_1 = 0.01, w_1 = 1, w_2 = 1, w_3 = 1, w_4 = 1 and w_5 = 1. Trajectories of components of $\mathbf{F}_{32}$ and $\mathbf{T}_{32}$ are shown in Figs. 19 and 20.

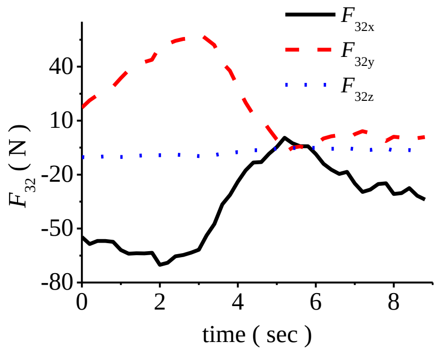

Fig. 19 Components of F_{32}

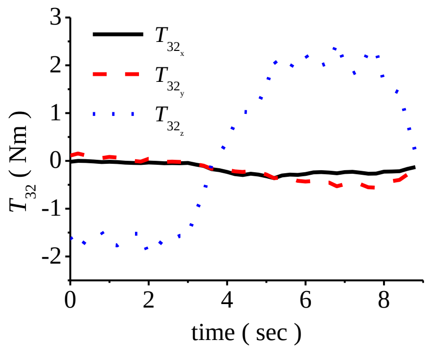

Fig. 20 Components of T_{32}

Compared with that of the three-actuator approach, the components of $\mathbf{T}_{32}$ are not always equal to zero which is quite consistent with kinesiology of the movement. Similarly, when the loads are increased to 1.5 and 2 folds one may find that magnitudes of $\mathbf{F}_{12}$ and $\mathbf{T}_{12}$ are increased proportionally as shown in Figs. 21 and 22. The results reveal that the multi-actuator approach yield trajectories of joint torque and force which obey the kinesiology of the upper limb movement. The results will be used in the next stage of muscle force sharing problem.

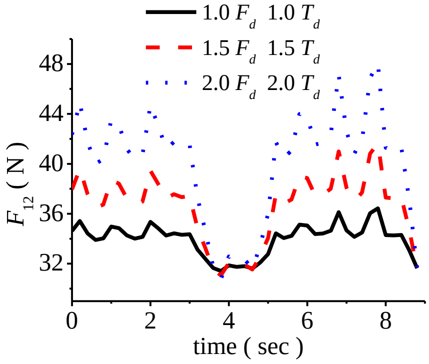

Fig. 21 Components of F_{12} with different loads

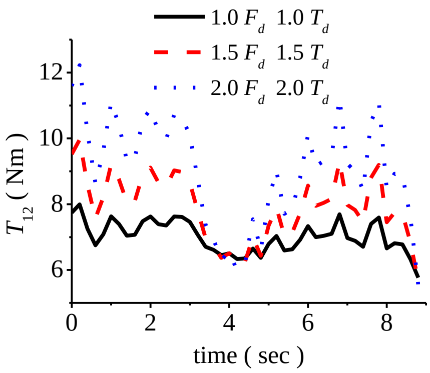

Fig. 22 Components of T_{12} with different loads

CONCLUSIONS AND SUGGESTIONS

Based on the proposed skeletal model of an upper limb driving a rehabilitation robot, a model for the displacement analysis is developed, and then two models for the force analysis are built. The followings are some remarks of the results:

(1) A spatial S-SUCr-U kinematic chain is proposed as the skeletal model between the shoulder and hand of an upper limb. When the upper arm of this skeletal model is held fixed, not only the elbow can do flexion motion, but the forearm is able to do the pronation and supination motions.
(2) Based on the proposed S-SUCr-U kinematic chain, the F_R-SUCr-S spatial four bar mechanism is proposed as the skeletal model of an upper limb driving a rehabilitation robot.
(3) The displacement analysis model of the F_R-SUCr-S spatial four bar mechanism is developed, and its correctness is verified by using the Adams software.
(4) The force analysis models of the F_R-SUCr-S spatial four bar mechanism with three inputs are developed, and their results are the same as those of using the Adams software.
(5) A quadratic programming model, for the force analysis of the F_R-SUCr-S four bar mechanism with all the joints been specified as inputs, is proposed.
(6) For each three-actuator force analysis approach, their results always exist unreasonable ones. Compare with them, those of using multiple actuator force analysis approach, with different loads, not only the forms of the curves of are all similar, respectively, but their magnitudes are all enlarged when the loads are increased, which are more reasonable.

Some suggestions for further studies of this subject are given in the followings:

(1) The proposed S-SUCr-U kinematic chain can be adopted as a basis to develop the skeletal model of an upper limb driving (or driven by) an equipment.
(2) The force analysis models are developed without considering the frictions and viscosities between the segments. They may be considered to get more precise results.
(3) The shoulder is assumed to be fixed in the developed models. The shoulder complex can be included to build a more complete skeletal model of an upper limb.
(4) Muscle systems can be included to develop the musculoskeletal model of an upper limb.

ACKNOWLEDGEMENT

The authors express their deep gratitude for the financial support of the National Science Council of Taiwan, NSC 98-2221-E-006 -039.

REFERENCES

Chen, C.-W., 2000, ”Development of a Robot for Neuro-Rehabilitation of Elbow,” Master Thesis, National Cheng Kung University, Tainan City, Taiwan.

Chen, Y.-C. and Chiou, S.-T., 2013a, ”A Closed Form Displacement Analysis of the Upper Extremity in Wheelchair Propulsion Using the RUUS Model,” The 16th National Conference on the Design of Mechanisms and Machines, Paper No.: conf-013_1, National Tsing Hua University, Hsinchu, Taiwan.

Chen, Y.-C. and Chiou, S.-T., 2013b, ”Optimal Motor Control of the Manual Wheelchair Propulsion with Upper Limbs Using the RUUS Model,” The 16th National Conference on the Design of Mechanisms and Machines, Paper No.: conf-013_2, National Tsing Hua University, Hsinchu, Taiwan.

Fazel-Rezai, R., Shwedyk, E., Onyshko, S., and Cooper, J. E., 1996, "Power Analysis of Upper Limb Movement," *Annual International Conference of the IEEE Engineering in Medicine and Biology - Proceedings*, Vol. 2, pp. 621-622.

Garner, B. A. and Pandy, M. G., 1999, "A Kinematic Model of the Upper Limb Based on the Visible Human Project Image Dataset," *Computer Methods in Biomechanics and Biomedical Engineering*, Vol. 2, pp. 107-124.

Gattamelata, D., Pezzuti, E., and Valentini, P. P., 2007, "Accurate Geometrical Constraints for the Computer Aided Modelling of the Human Upper Limb," *Computer-Aided Design*, Vol. 39, pp. 540-547.

Holzbaur, K. R. S., Murray, W. M., and Delp, S. L., 2005, "A Model of the Upper Extremity for Simulating Musculoskeletal Surgery and Analyzing Neuromuscular Control," *Annals of Biomedical Engineering*, Vol. 33, No. 6, pp. 829-840.

Kung, P.-C., Ju, M.-S., and Lin, C.-C. K., 2007, "Design of a Forearm Rehabilitation Robot," Proceedings of the 2007 IEEE 10th International Conference on Rehabilitation Robotics, June 12-15, Noordwijk, The Netherland, pp. 228-233.

Lemay, M. A., and Crago, P. E., 1996, "A Dynamic Model for Simulating Movements of the Elbow, Forearm, and Wrist," *Journal of Biomechanics*, Vol. 29, No. 10, pp. 1319-1330.

Liu, H.-C., 2011, ”An S- SUCr -U Skeleton Model and Its Applications on the Kinematic and Loading Analyses of the Upper Limb for Wheelchair Propulsion and Rehabilitation Robot Training,” Master Thesis, National Cheng Kung University, Tainan City, Taiwan.

Mercer, J. L., Boninger, M., Koontz, A., Ren, D., Dyson-Hudson, T., and Cooper, R., 2006, "Shoulder Joint Kinetics and Pathology in Manual Wheelchair Users," *Clinical Biomechanics*, Vol. 21, No. 8, pp. 781-789.

Nunome, H., Wataru, D., Shinji, S., Yasuo, I., and Kyonosuke, Y., 2002, "A Kinematic Study of the Upper-limb Motion of Wheelchair Basketball Shooting in Tetraplegic Adults," *Journal of Rehabilitation Research and Development*, Vol. 39, No. 1, pp. 63-71.

Pennestrì, E., Stefanelli, R., Valentini, P. P., and Vita, L., 2007, "Virtual Musculo-Skeletal Model for the Biomechanical Analysis of the Upper Limb," *Journal of Biomechanics*, Vol. 40, No. 6, pp. 1350-1361.

Shan, G., and Bohn, C., 2003, "Anthropometrical Data and Coefficients of Regression Related to Gender and Race," *Applied Ergonomics*, Vol. 34, No. 4, pp. 327-337.

Waldron, K. J., and Kinzel, G. L., 2004, *Kinematics*, Dynamics, *and Design of Machinery*, John Wiley & Sons, Inc., NJ, USA, pp. 18.

Wu, H.-W., 1998, “Biomechanics of Upper Extremity in Wheelchair Propulsion,” PhD Thesis, National Cheng Kung University, Tainan City, Taiwan.

Wu, H.-W., Berglund, L. J., Su, F.-C., Yu, B., Westreich, A., Kim, K.-J., and An, K.-N., 1998, "An Instrumented Wheel for Kinetic Analysis of Wheelchair Propulsion," *ASME Trans.*, *Journal of Biomechanical Engineering*, Vol. 120, pp. 533-535.

Wu, S.-Y., 2003, "Clinical Trials and Modification of Rehabilitation Robot for Upper Limbs," Master Thesis, National Cheng Kung University, Tainan City, Taiwan.

Zhou, H., Hu, H., and Tao, Y., 2006, "Inertial Measurements of Upper Limb Motion," *Medical and Biological Engineering and Computing*, Vol. 44, No. 6, pp. 479-487.

應用 F_R-SUCr-U 模型於上肢驅動復健機械手之運動及負荷分析

邱顯堂
國立成功大學機械工程學系

劉豪哲
日意機械股份有限公司研發部

朱銘祥
國立成功大學機械工程學系

林宙晴
國立成功大學醫學系神經部

摘要

本文的主要目的在於提出上肢的新骨骼模型並建立上肢驅動復健機械手的位移及負荷分析模式，以期有助於復健機械手等的研發。首先提出空間 S-SUCr-U 運動鏈，以模擬上肢肩關節至腕關節之間的新型骨骼模型，其特點為肱骨不動時能描述前臂旋前旋後的動作。再以此模型為基礎，提出空間 F_R-SUCr-S 四連桿機構，以模擬上肢驅動復健機械手的模型。接著針對此機構先建立其位移分析模式，再建立其負荷分析的兩種模式：三驅動模式及多驅動模式。為驗證模型的合理性，本研究以以上肢驅動復健機械手為實例，自行撰寫分析程式，而其解亦使用商用電腦輔助設計軟體所得結果驗證其正確性。比較三驅動與多驅動模式所得的負荷分析結果，發現使用多驅動模式所得的結果較合乎上肢動作的肌動學原理。本研究發展的新模型可以改善現有模型肱骨不動時，前臂無法旋前旋後的缺點。